Anal. Chem. **2009,** *81,* 443–452

Atmospheric Pressure Free Liquid Infrared MALDI Mass Spectrometry: Toward a combined ESI/MALDI-Liquid Chromatography Interface

Erdmann Rapp,*,† Aleš Charvát,*,‡ Alexander Beinsen,§ Uwe Plessmann,|| Udo Reichl,† Andreas Seidel-Morgenstern,† Henning Urlaub,|| and Bernd Abel§,⊥

Max Planck Institute for Dynamics of Complex Technical Systems, Sandtorstrasse 1, 39106 Magdeburg, Germany, Department of Photochemistry and Kinetics, Max Planck Institute for Biophysical Chemistry, Am Fassberg 11, 37077 Göttingen, Germany, Bioanalytical Mass Spectrometry Group, Max Planck Institute for Biophysical Chemistry, Am Fassberg 11, 37077 Göttingen, Germany, Institute for Physical Chemistry, Georg-August University of Göttingen, Tammannstrasse 6, 37077 Göttingen, Germany, W.-Ostwald-Institute for Physical and Theoretical Chemistry, University Leipzig, Linné-Strasse 2, D-04103 Leipzig, Germany

A new atmospheric pressure (AP)-MALDI-type interface has been developed based on a free liquid (FL) microbeam/microdroplets and a mid-infrared optical parametric oscillator (mid-IR OPO). The device is integrated into a standard on-line nanoESI interface. The generation of molecular ions in the gas phase is believed to be the result of a fast (explosive) laser-induced evaporative dispersion (not desorption) of the microbeam into statistically charged nanodroplets. Only the lowest charge states appear in significant abundance in this type of experiment. Mass spectra of some common peptides have been acquired in positive ion mode, and the limit-of-detection of this first prototype (liquid microbeam setup) was evaluated to be 17 fmol per second. To improve the duty cycle and to reduce the sample consumption, a droplet-on-demand system was implemented (generating 100 pL droplets). With this setup, about 20 attomole of bradykinin were sufficient to achieve a signal-to-noise ratio better than five. This setup can be operated at flow rates down to 100 nL/min and represents a liquid MALDI alternative to the nanoESI. Our particular interest was the application of the developed ion source for on-line coupling of liquid chromatography with mass spectrometry. The flow rates (>100 μL/min), required for stable operation of the ion source in continuous liquid microbeam mode, matches perfectly the flow rate range of microHPLC. Therefore, on-line LC/MS experiments have been realized, employing a microbore C18 reversed-phase column to separate an artificial peptide mixture and tryptic peptides of bovine serum albumin (performing a peptide mass fingerprint). In the latter case, sequence coverage of more than 90% has been achieved.

The analysis of biomolecules by mass spectrometry put rather severe constraints on the ionization method, as far as its ability to produce intact biomolecular ions (without uncontrollable fragmentation) is concerned. With the advent of the electrospray ionization (ESI)[1,2] and matrix-assisted laser desorption/ionization (MALDI),[3−5] two ionization sources of an unprecedented softness appeared. Because of the increasing need for powerful analytics of complex mixtures, the use of LC/MS (together with GC/MS), for example, in live sciences, airport surveillance, or food control is well established nowadays.[6−10]

Concomitantly, coupling of separation methods, such as high-performance liquid chromatography (HPLC), with the mass spectrometric detection appeared prerequisite for dealing with complex mixtures of biomolecules, such as protein digests of cell lysates. The quest for the best LC/MS interface started early in the 1970s (cf. refs 11, 12 and references cited therein). Two main strategies have been pursued and developed.[13−15] First, the off-line LC/MS analysis,[14,16,17] where separation and MS acquisition are decoupled. The freedom of optimizing both steps independently is offset to some extent by increased expenditure of time. Second, in on-line LC/MS coupling the eluted chromatographic fractions are conducted directly into the ion source of the mass

* To whom correspondence should be addressed. E-mail: rapp@mpi-magdeburg.mpg.de (E.R.), acharva@gwdg.de (A.C.). Fax: +49-391-6110 535 (E.R.), +49-551-2011 501 (A.C.).

† Max Planck Institute for Dynamics of Complex Technical Systems.

‡ Department of Photochemistry and Kinetics, Max Planck Institute for Biophysical Chemistry.

§ Georg-August University of Göttingen.

|| Bioanalytical Mass Spectrometry Group, Max Planck Institute for Biophysical Chemistry.

⊥ University Leipzig.

(1) Fenn, J. B.; Mann, M.; Meng, C. K.; Wong, F. S.; Whitehouse, C. M. *Science* **1989**, *246*, 64–71.
(2) Cole, R. B., Ed. *Electrospray Ionization Mass Spectrometry*; John Wiley & Sons: New York, 1997.
(3) Karas, M.; Hillenkamp, F. *Anal. Chem.* **1988**, *60*, 2299–2301.
(4) Tanaka, K.; Waki, H.; Ido, Y.; Akita, S.; Yoshida, Y.; Yoshida, T. *Rapid Commun. Mass Spectrom.* **1988**, *2*, 151–153.
(5) *MALDI MS: A Practical Guide to Instrumentation, Methods and Applications*; Hillenkamp, F., Peter-Katalinic, J., Eds.; Wiley-VCH: New York, 2007.
(6) *Principles of Mass Spectrometry Applied to Biomolecules*; Laskin, J., Lifshitz, C., Eds.; Wiley-Interscience: New York, 2006.
(7) Kaltashov, I. G.; Eyles, S. J. *Mass Spectrometry in Biophysics: Conformation and Dynamics of Biomolecules*; John Wiley & Sons Inc.: Hoboken, 2005.
(8) Pramanik, B. N.; Ganguly, A. K.; Gross, M. L. *Applied Electrospray Mass Spectrometry*; Marcel Dekker: Basel, 2002.
(9) *Identification of Microorganisms by Mass Spectrometry*; Wilkins, C. L., Jackson, O. L. J., Eds.; John Wiley & Sons: Hoboken, 2006.
(10) *Mass Spectrometry in Medicinal Chemistry*; Wanner, K. T.; Höfner, G., Eds.; Wiley-VCH: New York, 2007.
(11) Abian, J. *J. Mass Spectrom.* **1999**, *34*, 157–168.
(12) Ardrey, B. *Liquid Chromatography - Mass Spectrometry: an Introduction*; John Wiley & Sons Ltd: Chichester, 2003.
(13) Gelpi, E. *J. Chromatogr. A* **1995**, *703*, 59–80.
(14) Murray, K. K. *Mass Spectrom. Rev.* **1997**, *16*, 283–299.
(15) Gelpi, E. *J. Mass Spectrom.* **2002**, *37*, 241–253.
(16) Hattan, S. J.; Parker, K. C. *Anal. Chem.* **2006**, *78*, 7986–7996.
(17) Young, J. B.; Li, L. *Anal. Chem.* **2007**, *79*, 5927–5934.

10.1021/ac801863p CCC: $40.75
Published on Web 12/08/2008

spectrometer.[15] While interfacing ESI on-line to LC is straightforward and ubiquitous, the possibility of doing so with MALDI is still absent in all commercial systems at this time.[18] Even though, several approaches already appeared to tackle this problem: An aerosol vacuum UV MALDI interface was presented by Murray et al.[19] On the basis of the continuous flow (CF) UV-MALDI developed by Li et al.,[20,21] Murray and co-workers reported on a CF IR-MALDI LC-interface employing a syringe pump to deliver the analyte to a stainless steel frit in a vacuum held at high voltage (20 kV).[22] Alternatively, working at ambient pressure, an AP-MALDI interface was developed for this purpose by Laiko et al.[23] Recently, they presented the results obtained with AP-IR-MALDI where the sample was spotted as droplet on target plate held at 2 kV.[24]

Apart from atmospheric pressure photoionization (APPI)[25] and atmospheric pressure laser ionization (APLI),[26] Zenobi and co-workers[27] have shown an on-line coupling of HPLC equipment with an atmospheric pressure interface using both UV and IR lasers and flow-injected samples (i.e., with no chromatographic separation), with no applied voltage to the sample. In the case of UV excitation, a UV-matrix (HCCA) and LC mobile phase were mixed in a T-piece, and a small droplet formed at the end of the exit capillary was irradiated by the laser light. MS detection was done on an orthogonal-injection TOF (Agilent). In the latter case (i.e., IR), a substantially modified AP-MALDI source (MassTech) and a LCQ Classic QIT mass spectrometer (Thermo Finnigan) were employed. A piezo-driven flow-through cell generated droplets on-demand with approximately 50 μm diameter which were irradiated by a focused IR light. No additional matrix was needed, as the mobile phase itself (water or water/glycerol) absorbed strongly at wavelengths around 3 μm.

The intriguing fact, that is, production of ions upon irradiating a liquid target with a strongly absorbing IR laser, is a well-known (but still not completely understood) phenomenon observed for the first time more than 10 years ago by Brutschy and collaborators[28] upon irradiating a liquid microbeam containing gramicidin D in a vacuum with a CO_2 laser (see also the discussion in ref 29 concerning ice as a matrix for IR MALDI MS). Up to now his and few other research groups[30−32] have been working on using and advancing this technique (abbreviated LILBID MS, laser-induced liquid beam ionization/desorption by Brutschy,[33] or free liquid (FL)-IR-MALDI MS by us[34]). Since its introduction, the use of HPLC equipment (e.g., pumps and injection valves) and nanosecond mid-IR optical parametric oscillators (OPO) have been proven to be very useful. Mass spectra of different types of molecules [35−37] and noncovalently bound complexes [38−40] have been obtained. Moreover, time-resolved kinetic studies of protein aggregation[41] or biomolecule's alteration under conditions of oxidative stress[34] have been addressed using this technique. In addition, an on-line coupling with a simple isocratic chromatographic separation of cyclodextrins on a C18 reversed-phase column has been recently reported.[34] These have been all-vacuum experiments. The liquid microbeam with diameter of 10 to 20 μm was placed either directly between acceleration plates of a time-of-flight (TOF) mass spectrometer,[28,30] or in a separate vacuum chamber outside of the mass spectrometer. In the latter case, ions were allowed to pass into the acceleration region of a TOF instrument by using a restrictive aperture ("sample cone").[42] A droplet-on-demand version (still with the desorption/ionization step in vacuo) with extremely low sample consumption in the attomole range of the LILBID apparatus has been described lately by Morgner et al.[43] Yet, a serious drawback of all these liquid beam experiments was the modest mass resolution achieved (~1000 at m/z~1000, and significantly lower toward higher m/z). The main reason for that is believed to be both the high initial velocities of ions, as well as the broad velocity distribution. Unlike MALDI,[44] unfortunately, this could be improved to only small extent by using delayed extraction.

This work highlights our efforts toward a unified ESI/liquid MALDI-type interface working at ambient conditions. The approach we have chosen consists in replacing the on-line nanoESI ion source of a commercial mass spectrometer by the novel Atmospheric Pressure Free Liquid Infrared Matrix-Assisted Laser *Dispersion* Ionization (AP-FL-IR-MALDI) interface (rapid switching between vacuum MALDI and ESI mode of operation on a Qq-TOF instrument (Sciex) was described in ref 45). This interface is based on our FL-IR-MALDI technique[34] but operating at ambient pressure. Obviously, operating such an ion source at atmospheric

(18) Hu, L.; Ye, M.; Jiang, X.; Feng, S.; Zou, H. *Anal. Chim. Acta* **2007**, *598*, 193–204.
(19) Murray, K. K.; Lewis, T. M.; Beeson, M. D.; Russell, D. H. *Anal. Chem.* **1994**, *66*, 1601–1609.
(20) Li, L.; Wang, A. P. L.; Coulson, L. D. *Anal. Chem.* **1993**, *65*, 493–495.
(21) Nagra, D. S.; Li, L. *J. Chromatogr. A* **1995**, *711*, 235–245.
(22) Lawson, S. J.; Murray, K. K. *Rapid Commun. Mass Spectrom.* **2000**, *14*, 129–134.
(23) Laiko, V. V.; Baldwin, M. A.; Burlingame, A. L. *Anal. Chem.* **2000**, *72*, 652–657.
(24) Laiko, V. V.; Taranenko, N. I.; Berkout, V. D.; Yakshin, M. A.; Prasad, C. R.; Sang Lee, H.; Doroshenko, V. M. *J. Am. Soc. Mass Spectrom.* **2002**, *13*, 354–361.
(25) Robb, D. B.; Covey, T. R.; Bruins, A. P. *Anal. Chem.* **2000**, *72*, 3653–3659.
(26) Constapel, M.; Schellenträger, M.; Schmitz, O. J.; Gäb, S.; Brockmann, K. J.; Giese, R.; Benter, T. *Rapid Commun. Mass Spectrom.* **2005**, *19*, 326–336.
(27) Daniel, J. M.; Laiko, V. V.; Doroshenko, V. M.; Zenobi, R. *Anal. Bioanal. Chem.* **2005**, *383*, 895–902.
(28) Kleinekofort, W.; Avdiev, J.; Brutschy, B. *Int. J. Mass Spectrom. Ion Processes* **1996**, *152*, 135–142.
(29) Berkenkamp, S.; Karas, M.; Hillenkamp, F. *Proc. Natl. Acad. Sci. U.S.A.* **1996**, *93*, 7003–7007.
(30) Horimoto, N.; Kohno, J.; Mafune, F.; Kondow, T. *J. Phys. Chem, A* **1999**, *103*, 9569–9572.
(31) Charvat, A.; Lugovoj, E.; Faubel, M.; Abel, B. *Eur. Phys. J. D* **2002**, *20*, 573–582.
(32) Otten, D. E.; Trevitt, A. J.; Nichols, B. D.; Metha, G. F.; Buntine, M. A. *J. Phys. Chem, A* **2003**, *107*, 6130–6135.
(33) Kleinekofort, W.; Pfenninger, A.; Plomer, T.; Griesinger, C.; Brutschy, B. *Int. J. Mass Spectrom. Ion Processes* **1996**, *156*, 195–202.
(34) Charvat, A.; Abel, B. *Phys. Chem. Chem. Phys.* **2007**, *9*, 3335–3360.
(35) Sobott, F.; Kleinekofort, W.; Brutschy, B. *Anal. Chem.* **1997**, *69*, 3587–3594.
(36) Sobott, F.; Wattenberg, A.; Barth, H.-D.; Brutschy, B. *Int. J. Mass Spectrom.* **1999**, *185−187*, 271–279.
(37) Abel, B.; Charvat, A.; Diederichsen, U.; Faubel, M.; Girmann, B.; Niemeyer, J.; Zeeck, A. *Int. J. Mass Spectrom.* **2005**, *243*, 177–188.
(38) Kleinekofort, W.; Schweitzer, M.; Engels, J. W.; Brutschy, B. *Int. J. Mass Spectrom. Ion Processes* **1997**, *163*, 1L−4L.
(39) Wattenberg, A.; Sobott, F.; Brutschy, B. *Rapid Commun. Mass Spectrom.* **2000**, *14*, 859–861.
(40) Wattenberg, A.; Sobott, F.; Barth, H.-D.; Brutschy, B. *Int. J. Mass Spectrom.* **2000**, *203*, 49–57.
(41) Charvat, A.; Bögehold, A.; Abel, B. *Aust. J. Chem.* **2006**, *59*, 81–103.
(42) Charvat, A.; Lugovoj, E.; Faubel, M.; Abel, B. *Rev. Sci. Instrum.* **2004**, *75*, 1209–1218.
(43) Morgner, N.; Barth, H.-D.; Brutschy, B. *Aust. J. Chem.* **2006**, *59*, 109–114.
(44) Jensen, O. N.; Podtelejnikov, A.; Mann, M. *Rapid Commun. Mass Spectrom.* **1996**, *10*, 1371–1378.
(45) Krutchinsky, A. N.; Zhang, W.; Chait, B. T. *J. Am. Soc. Mass Spectrom.* **2000**, *11*, 493–504.

pressure is much more user-friendly compared to the previous vacuum operation. In addition, the surrounding gas molecules efficiently thermalize, and thereby equalize the widespread and high initial velocities (up to several km per second[46]) of ions or ionic aggregates after being ejected from the liquid beam in a sort of a phase explosion.[47] However, the question of an efficient ion transfer from atmospheric pressure into the vacuum of the mass spectrometer may still be an important issue.

For the liquid microbeam setup only minor modifications had to be implemented to enable ion generation by intercepting the continuous liquid filament in front of the orifice with the focused optical radiation of an IR OPO. We found that ES emitters originally designed and manufactured for nanoESI are also well suited for the generation of free liquid microbeams (at flow rates greater than ~100 μL/min). Such an interface enables to operate the mass spectrometer with different ion sources using the same hardware. In addition, switching between, for example, nanoESI MS (high voltage on, laser off, low flow rate) and AP-FL-IR-MALDI MS (high voltage off, laser on high flow rate), can be readily done on a minute time scale. Hybrid experiments, such as laser spray,[48] ELDI (Electrospray-assisted Laser Desorption/ Ionization),[49] MALDESI (Matrix-assisted Laser Desorption Electrospray Ionization),[50] LAESI (Laser Ablation Electrospray Ionization),[51] or IR LADESI (Laser-assisted Desorption Electrospray Ionization),[52] could be conducted as well utilizing the new interface.

In this paper, the performance of the first prototype of an AP-FL-IR-MALDI mass spectrometer is presented. In the first part of the manuscript, two setups are investigated by a set of common peptides (penta- to tridecapeptides) in positive ion mode: the liquid microbeam setup (operating in continuous microbeam mode) and the droplets-on-demand setup (operating in microdroplets on demand mode). Sensitivity and the limit of detection for both modes of the AP-FL-IR-MALDI interface are highlighted and discussed. The second part of the paper deals with the feasibility of the novel interface for on-line coupling of HPLC with MS. This has been demonstrated by using the continuous microbeam mode conducting microHPLC MS (μHPLC MS) separations of an artificial peptide mixture, as well as of tryptic peptides of bovine serum albumin (BSA). Both separations were acquired in the single MS mode. In the latter case, using protein database searching algorithms, the generated peptide mass fingerprint (PMF) showed sequence coverage of more than 90%. To have some direct point of reference, the analysis was repeated just by switching to the nanoHPLC nanoESI MS setup, running the same sample onto the same mass spectrometer.

EXPERIMENTAL SECTION

All solvents and chemicals, not particularly mentioned in the following (and within the Supporting Information), were of analytical grade or higher and were purchased from Fluka/Riedel-de Haën/Sigma-Aldrich (Taufkirchen, Germany), or Merck VWR (Darmstadt, Germany), respectively. Pure deionized water was always prepared freshly by bi-distillation or via a Millipore-Direct Q5 system (Millipore, Schwalbach, Germany).

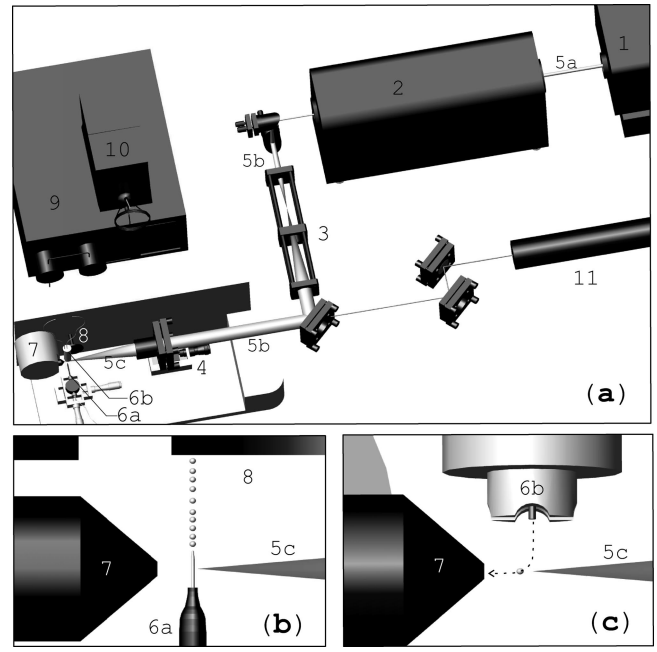

Figure 1. (a) Drawing of the experimental arrangement: (1) Nd:YAG pump laser, (2) OPO, (3) telescope, (4) focusing lens, (5a) pulsed NIR laser-beam (wavelength 1064 nm) generated by a 20 Hz Nd:YAG laser, (5b) pulsed mid-IR laser-beam (wavelength 2.9 μm) generated by the OPO, (5c) pulsed mid-IR laser-beam, focused to roughly 100 μm in diameter, hitting the continuous liquid beam respectively, the single microdroplets directly in front of the orifice of the sample cone, (6a) microbeam nozzle, (6b) microdroplet dispenser, (7) entrance skimmer of the mass spectrometer (sample cone), and (8) the grounded electrode of the mass spectrometer (baffle). (9) HPLC pump, (10) injection valve with sample loop, and (11) He−Ne laser using for adjustment are also displayed. (b) Top view of the sample cone region depicting the liquid microbeam setup, operating in continuous microbeam mode. The laser radiation is focused onto the liquid filament. (c) Side view of the sample cone region depicting the droplet-on-demand setup, operating in microdroplet on demand mode. Single droplets, getting suctioned toward the orifice (caused by the vacuum behind) are ablated by absorbing laser radiation directly in front of the orifice.

AP-FL-IR-MALDI. *MS Instrumentation.* The ion source of a Q-Tof Ultima API mass spectrometer (Micromass, Waters Corporation, Manchester, U.K.) was operated at 0 kV capillary voltage and cone voltage of 122 V (program setting 55). Other important settings and parameters are listed in Table S-1, Supporting Information. They were kept constant during all experiments. Acquired chromatograms and related spectra were processed by the MassLynx software (Version 4.0, Micromass), extracted as ASCII data files and plotted using Origin (version 7.0, OriginLab).

Sample Delivery System. (**a**) Flow injection of the analyte molecules was realized with a 100 μL PEEK sample loop attached to an injection valve (model MX9925, Rheodyne, Rohnert Park, CA). An uncoated fused-silica Silicatip emitter (i.e.,nozzle) (360 × 75 μm o.d. × i.d., tip i.d. 15 μm, New Objective, Woburn, MA) was mounted on a three-axis manipulator in front of the mass spectrometer and connected with 1/16″ o.d. PEEK tubing to the outlet port of the injection valve. The tip-end (schematically shown in Figure 1b) was positioned tightly to the entrance orifice (sample

(46) Stasicki, B.; Charvat, A.; Faubel, M.; Abel, B. *Proc. SPIE* **2005**, *5580*, 335–346.
(47) Charvat, A.; Stasicki, B.; Abel, B. *J. Phys. Chem, A* **2006**, *110*, 3297–3306.
(48) Hiraoka, K.; Matsushita, F.; Huasawa, H. *Int. J. Mass Spectrom. Ion Processes* **1997**, *162*, 35–44.
(49) Shiea, J. T.; Huang, M. Z.; Hsu, H. J.; Lee, C. Y.; Yuan, C. H.; Beech, I.; Sunner, J. *Rapid Commun. Mass Spectrom.* **2005**, *19*, 3701–3704.
(50) Sampson, J. S.; Hawkridge, A. M.; Muddiman, D. C. *J. Am. Soc. Mass Spectrom.* **2006**, *17*, 1712–1716.

cone) of the mass spectrometer (needle orthogonal to the entrance orifice axis). Powered by a HPLC pump (model 300C, Gynkotek/Dionex, Germering, Germany) with flow rates of 200−300 μL/min, a liquid beam was formed downstream the nozzle. The first, cylindrical, part of the liquid jet consists of an intact liquid beam with a few millimeters in length and a diameter of about 12 μm.[53] Downstream of this region, the liquid beam disintegrates into droplets because of the Rayleigh instability [54,55] (Figure 1b). The liquid/droplet stream was directed onto the grounded counter-electrode (baffle) of the mass spectrometer and collected in a waste bin (Figure 1b).

(**b**) A droplet-on-demand (DoD) system (microdrop Technologies GmbH, Norderstedt, Germany) was used to produce ~100 pL (50 μm in diameter) droplets at a repetition rate of 20 Hz. The droplets were allowed to move 2 mm at ambient pressure and were hit by the IR radiation in front of the orifice of the mass spectrometer (see Figure 1c). A digital delay generator (DG535, Stanford Research Systems, Sunnyvale, CA) was used to synchronize the droplet generation with the laser pulse.

Laser System. Figure 1a shows the laser and optical system used in the experiments. Infrared (IR) radiation has been generated in an optical parametric oscillator (OPO) (GWU-Lasertechnik, Erfstadt, Germany) equipped with a $KNbO_3$ crystal. OPO has been pumped by a 20 Hz Nd:YAG laser (Quanta-Ray Indi series, Newport Corporation-Spectra Physics, Mountain View, CA). The mid-IR optical radiation of idler beam (tunable between 2.6−3.1 μm) was steered by gold mirrors and directed through a magnifying telescope (magnification of 3) and a singlet focusing CaF_2 lens (100 mm focal length) onto the liquid target. The most suitable wavelength of the idler wave was found to be about 2.9 μm. Only slight variation of the laser energy from 2 to 3 mJ/pulse before the focusing lens was allowed.

Chromatographic Separation. The chromatographic separation of a tryptic digest corresponding to 7.5 pmol BSA was performed on SMART system (GE Healthcare Life Sciences, München, Germany) equipped with a 2.1 × 150 mm (i.d. × length) Vydac 218 TP5215 microbore C18 reversed-phase separation column (Alltech Grom/Grace Davison Discovery Sciences, Rottenburg-Hailfingen, Germany) and 50 μL sample loop running at a flow rate of 200 μL/min. The sample was desalted with a pre-column (Vydac, 2.1 mm i.d. × 7.5 mm L) mounted in line. The loop was loaded using 100 μL of the peptide solution. Solvents A and B were 0.1% aqueous formic acid (FA) and 0.1% solution of FA in acetonitrile (ACN), respectively. Alternatively, trifluoroacetic acid (TFA) in the same concentration was used. The separation was performed at room temperature with a gradient of 5 to 60% B within 24.5 min.

NanoESI MS Instrumentation and Chromatographic Separation. Q-Tof Ultima (Micromass, Waters Corporation) was operated in positive ion mode with the capillary and cone voltage settings of 2 kV and 55V. A standard distal coated Silicatip (360 × 20 μm o.d. × i.d., tip i.d. 10 μm, New Objective) was used as ES emitter. The chromatographic separation was carried out at a CapLC Unit (Waters) at 200 nL/min using a self-packed 75 μm × 150 mm (i.d. × length) capillary column containing ReproSil-Pur 120Å-C18-AQ-3 μm (Dr. Maisch GmbH, Ammerbuch-Entringen, Germany). Samples were desalted on a precolumn (LC Packings/Dionex Germering, Germany; 0.3 mm i.d. × 5 mm L) working in the back-flush mode. Solvent A consisted of 0.1% FA_{aq}, solvent B was a mixture of 80% (v/v) ACN: 0.1% FA_{aq}. A 40 min gradient (10−40%) B was applied. The amount of the tryptic digest corresponding to 100 fmol of BSA was loaded onto the column.

PMF Data Evaluation. For PMF-like data evaluation, the processed peak list containing measured centroid peaks (in each scan) was generated using the peak-picking algorithm DECON 2LS (http://ncrr.pnl.gov/software) for three different values of the background cutoff parameter, r (r = 6, 10, and 20 cps), and a signal-to-noise (S/N) ratio of (at least) 5. In addition, the m/z values (in laser-based experiments) were corrected by a parabolic polynomial function which was found to account well for the differences between calculated and observed masses of the flow-injected peptides (see Table S-2, Supporting Information). For identification, the peak list (note, peaks lower than 500 m/z were omitted) was searched against NCBI non-redundant database (09.01.2008) using MASCOT (version 2.2, Matrix Science, London, U.K.) as search engine.[56] The available taxonomic search space was used without restriction. For the search, two missed tryptic cleavages were allowed and the monoisotopic m/z tolerance was set to ± 150 ppm. Retrieved mass peaks lower than 500 m/z were omitted. Two search types were accomplished. First, only alkylation of cysteine residues with iodoacetamide (carbamidomethyl(C)) was selected and set as a *fixed* modification (Table 1). Second, the search with following *variable* modifications was performed: carbamidomethyl(C), carbamyl(K), because of urea used in the preparation of the BSA digest,[57] and oxidation(M) (Table 2).

Chemicals and Sample Preparation. All peptides (leucine-enkephalin (Leu-Enk), methionine-enkephalin (Met-Enk), angiotensin I (AngI), angiotensin II (AngII), bradykinin (Brad), neurotensin (Neu), and the sex pheromone inhibitor (iPD1)) were obtained from Bachem (Bachem Distribution Services GmbH, Weil am Rhein, Germany, cf. Table S-2, Supporting Information) and used without further purification. The day-to-day system checkup and/or optimization procedure was performed with 0.5 μM solution of indole alkaloid reserpine (Sigma-Aldrich, cf. Table S-2, Supporting Information) in 0.1% FA_{aq}. Amino acid sequences of the peptides are summarized in Table S-2, Supporting Information. Stock solutions of peptides (in the 10−100 mM range) were prepared for all but two (Met-Enk and iPD1) by adding 500 μL of 0.1% FA_{aq}/ACN (1:1, v/v) solution to the peptide's vial, followed by 10 min of sonication; Met-Enk was dissolved in 5 mL, whereas iPD1 had to be dissolved in 10 mL of the solvent. Out of these stock solutions several hundreds of microliters of 100 μM solutions of each peptide were made and used as a starting point for further dilutions. For the dilution a stock solution of 0.1% FA in H_2O/ACN (1:1, v/v) was used. The pH value of the injected peptide samples was about 3. A 3 pmol/μL storage stock solution of tryptic digested BSA (Pierce(Perbio Science)/ThermoFisher Scientific, Bonn, Ger-

(51) Nemes, P.; Vertes, A. *Anal. Chem.* **2007**, *79*, 8098–8106.
(52) Rezenom, Y. H.; Dong, J.; Murray, K. K. *Analyst* **2008**, *133*, 226–232.
(53) Faubel, M. In *Photoionization and Photodetachement*; Ng, C.-Y., Ed.; World Scientific Publishing Co.: Singapore, 2000; Vol. 1, pp 634−689.
(54) Rayleigh, Lord. *Proc. London Math. Soc.* **1879**, *10*, 4.
(55) Rayleigh, Lord. *Philos. Mag.* **1892**, *34*, 145.
(56) Perkins, D. N.; Pappin, D. J. C.; Creasy, D. M.; Cottrell, J. S. *Electrophoresis* **1999**, *20*, 3551–3567.

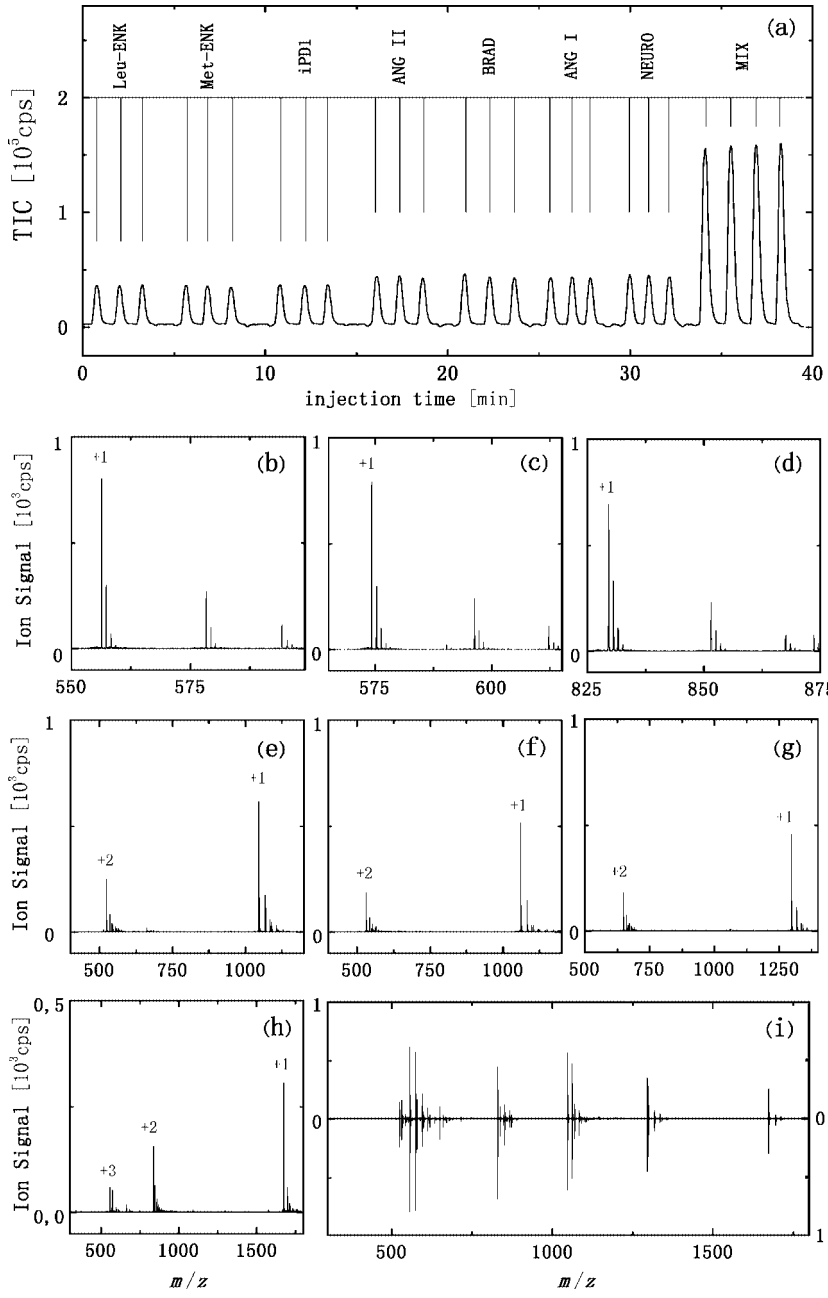

Figure 2. (a) Total ion current of flow-injected samples. Mass spectra of (b) leucine-enkephalin, (c) methionine-enkephalin, (d) iPD1, (e) angiotensin II, (f) bradykinin, (g) angiotensin I, and (h) neurotensin. (i) Comparison of mass spectra of an equimolar peptide mixture (upper trace) and a merged sum of individually injected peptides (i.e., (b)−(h), mirrored lower trace).

many; cf. Table S-2, Supporting Information) was prepared in house (aliquoted and stored at −80 °C). The detailed digestion protocol is given on-line as Supplementary Note 1, Supporting Information. If required, a 1.5 μM working stock solution (1.5 pmol/μL) of tryptically digested BSA was prepared freshly, just adding 0.1% FA_{aq} 1:1 to the thawed aliquots.

RESULTS AND DISCUSSION

Interface Characterization I: Liquid Microbeam Setup (Operating in Continuous Microbeam Mode). Figure 2a shows the total ion current (TIC) trace of flow injected samples of 1 μM peptide solutions. Raw mass spectra displayed have been acquired within 1 s representing an average of 20 laser pulses (i.e., 4 pmol of the analyte consumed). The 100 μL sample loop was always flushed with 200 μL of the sample solution. In general, the single-charge protonated species appears as the most abundant pseudomolecular ion, accompanied by a set of weaker cluster ions with sodium and potassium because of some cationic impurities (e.g., salts see Figure 2b−d). For peptides with masses above approximately 1 kDa, additionally higher charged states (+2, +3) occur (cf. Figure 2e−h), although their intensity stays always well below that of the single-charge ion (about 30−50% thereof). Mass resolution ($m/\Delta m$) of 9000 has been achieved throughout the mass range covered in the experiment. Comparing the peptide mixture with the merged sum of individual peptide spectra (Figure 2i) reveals a very good agreement. The overall intensity of the mixture is somewhat lower but the ratio of abundances of

Table 1. PMF Protein Identification - Fixed Modification[a]

μHPLC AP-FL-IR-MALDI MS	r [cps]	no. queries	carbamidomethyl(C) no. matched (η)	MOWSE score	sequence coverage [%]
7.5 pmol	6	129	54 (*0.42*)	331	71
	10	62	37 (*0.60*)	297	51
	20	23	21 (*0.91*)	247	31
37.5 pmol	6	289	70 (*0.24*)	258	88
	10	133	53 (*0.40*)	322	74
	20	53	34 (*0.64*)	308	59
in silico[b]		238	220 (*0.92*)	1020	98
		238	236 (*0.99*)	1020	100

[a] Peak-picking and deconvolution using DECON 2LS (see also refs : Horn, D. M.; Zubarev, R. A.; McLafferty, F. W. *J. Am. Soc. Mass Spectrom.* **2000**, *11*, 320−332; Zimmer, J. S. D.; Monroe, M. E.; Qian, W.-J.; Smith, R. D. *Mass Spectrom. Rev.* **2006**, *25*, 450−482); Settings: S/N = 5, peak-fit type - quadratic; Horn transform − THRASH; Savitzky-Golay smoothing − order 2. [b] in silico data generated for two missed cleavages with no (post-translational, chemical) modifications. The first row corresponds to albumin [*Bos taurus*] (gi|30794280), while the second to serum albumin precursor (gi|1351907).

Table 2. PMF Protein Identification - Variable Modifications[a]

μHPLC AP-FL-IR-MALDI MS	r [cps]	no. queries	carbamidomethyl(C), carbamyl(K), and oxidation(M) no. matched (η)	MOWSE score	sequence coverage [%]
7.5 pmol	6	129	86 (*0.67*)	216	79
	10	62	48 (*0.77*)	203	58
	20	23	22 (*0.96*)	152	31
37.5pmol	6	289	148 (*0.51*)	92	93
	10	133	95 (*0.71*)	234	81
	20	53	47 (*0.89*)	224	57

[a] cf. legend of Table 1.

different peptides has been conserved to a large extent, namely, the analyte interference seems to be virtually absent in this case.

Despite the large variety of experimental conditions encountered in the literature, a comparison of the present findings to those acquired with other MS techniques can be done on a qualitative basis. As already established in vacuum experiments[28] the appearance of singly charged species is predominant. On the other hand, ESI experiments dealing with the same molecules generally report on higher charge states being the most abundant.[58−60] Neither AP-FL-IR-MALDI mass spectra nor ESI mass spectra, however, represent a true image of the (estimated) protonation equilibria in solution. A large disparity exists between them and measured mass spectra.[61] In contrast to AP-FL-IR-MALDI MS (where charge states higher than unity are observed), for AP-[24] and vacuum-[62] MALDI MS an almost negligible occurrence of higher charge states (larger than +1) has been reported for almost the same set of peptides.

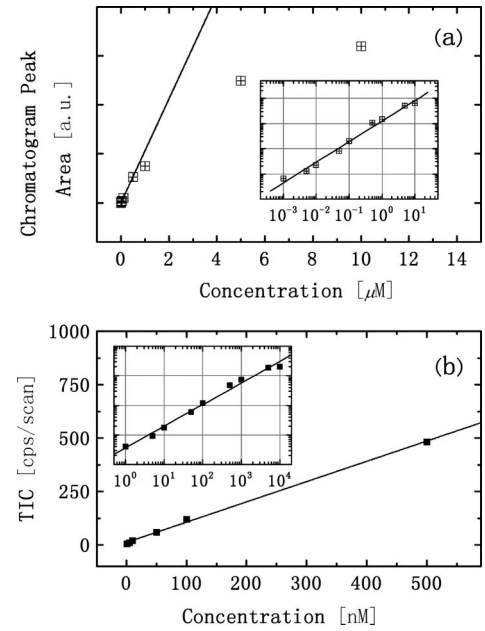

Figure 3. (a) Chromatogram peak areas of the XIC trace (m/z = 1060 ± 2) of flow injected bradykinin pulses (100 μL injected at a flow rate of 200 μL/min), depicted as a function of the concentration. The inset shows the same dependence on a log−log scale. (b) Dependence of TIC at m/z 1060.5 on the sample concentration for 1 scan of 1 s duration. Functional dependence of the linear fit: TIC = 9.56(±4.1) + 0.95(±0.02) × c (R = 0.99925). In the inset, TIC versus concentration on a log−log scale is shown.

Bradykinin, a physiologically and pharmacologically active octapeptide with a molecular mass of 1059.56 Da, has been chosen for the determination of the linearity range and the limit of detection (LOD). In Figure S-1, Supporting Information, the extracted ion chromatograms (XIC) of concentration series for bradykinin are shown. Starting at the lowest concentration, sample concentration was increased stepwise, doing repeated flow injections on every concentration stage. Also, blank mobile phase injections were performed at the beginning of each run to verify that there was no carryover. The chromatographic peak area as a function of the concentration is plotted in Figure 3a. Each point is an average of all injections measured at a particular concentration. Exceeding roughly 500 nM, the ion signal starts to deviate obviously from a straight line. The same dependence has also been observed when the maximum TIC in one scan was evaluated as a function of bradykinin concentration. Here the ion signal leveling-off occurs for TIC rates above roughly 700 cps. Such a behavior is the result of the limited linear dynamic range of the time-to-digital converter (TDC) implemented in the Q-Tof mass spectrometer. A linear regression in the lower concentration range (1−500 nM) seems to fit more than satisfactorily to experimental data (correlation coefficient, R > 0.999, Figure 3b). In Figure 3 both insets suggest, that on a log−log scale even the whole set of data points can be reasonably fitted with an "average" slope of about 0.75(±0.05) (R = 0.995).

(57) McCarthy, J.; Hopwood, F.; Oxley, D.; Laver, M.; Castagna, A.; Righetti, P. G.; Williams, K.; Herbert, B. *J. Proteome Res.* **2003**, *2*, 239–242.
(58) Andren, P. E.; Emmett, M. R.; Caprioli, R. M. *J. Am. Soc. Mass Spectrom.* **1994**, *5*, 867–869.
(59) Schnier, P. D.; Gross, D. S.; Williams, E. R. *J. Am. Soc. Mass Spectrom.* **1995**, *6*, 1086–1097.
(60) Iavarone, A. T.; Jurchen, J. C.; Williams, E. R. *Anal. Chem.* **2001**, *73*, 1455–1460.
(61) Wang, G.; Cole, R. B. *Org. Mass Spectrom.* **1994**, *29*, 419–427.
(62) Cohen, L. H.; Gusev, A. I. *Anal. Bioanal. Chem.* **2002**, *373*, 571–586.
(63) Mueller, M.; Gornushkin, I. B.; Florek, S.; Mory, D.; Panne, U. *Anal. Chem.* **2007**, *79*, 4419–4426.

The LOD for flow injection analysis of bradykinin is based on the estimate,[63] LOD $\equiv 3\sigma_B/\alpha$, where σ_B describes the standard deviation of the background noise and α corresponds to the slope of the linear fitting curve in Figure 3b. Hence, taking $\sigma_B \sim 2$ (evaluated for $1000 < m/z < 1050$), and $\alpha \sim 1$, the LOD equals approximately 5 nM solution (i.e., at a flow rate of 200 μL/min 16.7 fmol per 1 s scan of the substance is consumed). The linear dynamic range spans thus 2 orders of magnitude from 5 to 500 nM. Let us emphasize that this dynamic range refers to a concentration range where a strict linearity (i.e., on a log−log scale having the slope equal to unity) between concentration and TIC is assured. Adopting, however, a more relaxed interpretation of dynamic range, the data presented on a logarithmic scale (Figure 3b) would suggest that the dynamic range even spans about 4 orders of magnitude (as suggested, e.g., in ref 51).

Extension of the linear dynamic range to both lower as well as higher concentrations can be realized. Currently, all experiments utilizing the continuous microbeam mode are performed with a laser of low repetition rate (i.e., 20 Hz). Consequently, the duty cycle of the interface with the liquid microbeam setup is rather low, as the continuously streaming liquid is hit (and the ions generated) only 20-times per second. However, the high flow velocity of the liquid microbeam (typically, 10−50m/s) would allow for a high-repetition laser with repetition rates above 1kHz. In such a way the duty cycle would be increased and therefore the potential of the MS instrument could be better exploited. Thus for instance, already the utilization of a laser with a repetition rate of 1kHz would improve the duty cycle by a factor of 50 with respect to the present experiment, and should result in a significantly lower LOD. About a 7-fold ($=\sqrt{50}$) decrease of LOD could be expected, assuming the baseline noise is of statistical nature. Another strategy to reduce LOD could consist in the enhancement of the ion transfer efficiency from the source to the mass spectrometer. In particular, the incorporation of a Venturi device proved helpful by raising significantly the ion transport efficiency from the high pressure region of the ion source into the vacuum of the mass analyzer.[64] The incorporation of such a device was demonstrated for an 18-fold increase of reserpine signal.[64] In addition, improvement of desolvation by using high-velocity gas flow occurring in an air amplifier was shown by Cooks and coworkers.[65]

As already mentioned, extending the linear dynamic range toward higher concentrations could be accomplished upon using an MCP detector in combination with either a fast analog-to-digital converter (ADC) or a multianode time-to-digital converter (MA-TDC).[66] The saturation of the signal observed in the present study can be mostly explained by the use of a traditional TDC, which is known to be "upper dynamic range-limited".[67] Indeed, a much broader linearity range (for concentrations up to 100 mM) using a reflectron TOF is already established in the vacuum variant of this method adopting the ADC detecting scheme.[37,43,68]

Interface Characterization II: Droplet-on-Demand Setup (Operating in Microdroplets on Demand Mode). As far as the sample consumption is concerned, the use of a droplet-on-demand generator seems to be the ultimate solution to this issue, as its duty cycle equals unity. For microdroplets smaller than 100 μm the most robust DoD-dispensers (showing least jitter) are those using piezo elements. Adjusting the delay between laser pulse and piezo-actuator allowed the laser radiation to hit the droplets in the nearest vicinity of the sample cone, which was not possible using the liquid microbeam setup. Furthermore, the droplets are now generated synchronously with the laser, and the droplet-on-demand setup made up a liquid delivery system which could be readily operated at low flow rates of approximately 100 nL/min (e.g., 100 pL droplets at 20 Hz). Consequently, the waste of sample is massively reduced, and the LOD is lowered by several orders of magnitude. Indeed, the results obtained with the droplet-on-demand setup, appeared to be very promising.

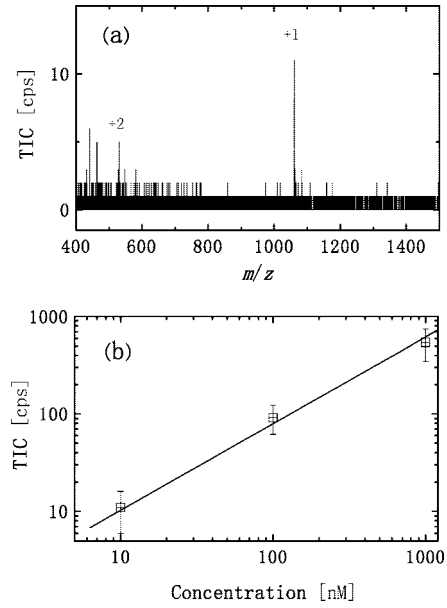

Figure 4. (a) Mass spectrum of 10 nM solution of bradykinin for one scan (20 droplets, 100 pl each) using the droplet-on-demand dispenser; 20 attomole of the sample were consumed. (b) Concentration dependence of TIC. The slope of the linear fit (on a log−log scale) equals 0.9.

Figure 4 summarizes the results obtained by AP-FL-IR-MALDI MS using a droplet-on-demand dispenser. In Figure 4a the mass spectrum of a 10 nM solution of bradykinin obtained with the DoD dispenser is displayed corresponding to a consumption of only 20 attomole of the analyte. Moreover, a nearly linear concentration dependence of TIC in Figure 4b (slope 0.9) shows once more that also this ion source provides the possibility for reliable quantitation. The relatively large error bars were mainly caused by the spatial jitter of the droplets because of air flow in the sample cone region. Conditions for optimized hydrodynamic focusing and enhanced spatial stability of droplets will be addressed in future experiments.

Regarding the feasibility of the interface for on-line coupling of HPLC with MS, especially with respect to miniaturization, the droplet-on-demand (DoD) dispenser setup, seems to perfectly match the needs of a nanoHPLC/MS. But the dead volume of

(64) Zhou, L.; Yue, B.; Dearden, D. V.; Lee, E. D.; Rockwood, A. L.; Lee, M. L. *Anal. Chem.* **2003**, *75*, 5978–5983.
(65) Yang, P.; Cooks, R. G.; Ouyang, Z.; Hawkridge, A. M.; Muddiman, D. C. *Anal. Chem.* **2005**, *77*, 6174–6183.
(66) LECO; Corporation *Separation Science Performance Note* 2005, 209−076−022.
(67) Guilhaus, M. *J. Mass Spectrom.* **1995**, *30*, 1519–1532.
(68) Charvat, A.; Gessler, F.; Niemeyer, J.; Boegehold, A.; Abel, B. *Anal. Lett.* **2006**, *39*, 2191–2203.

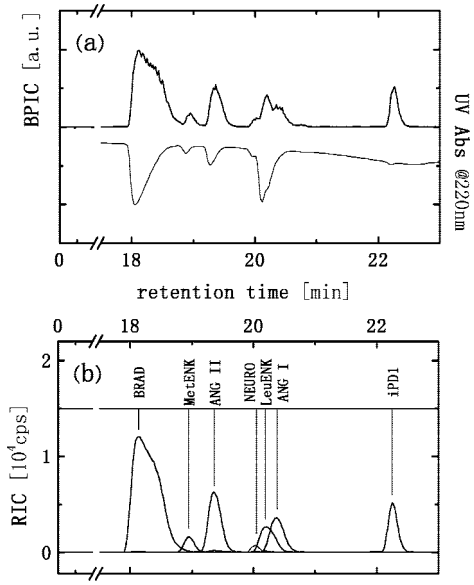

Figure 5. μHPLC AP-FL-IR-MALDI MS and UV of peptide mixture. (a) BPIC (upper trace) and absorbance at 220 nm (mirrored lower trace). (b) RIC of eluted peptides.

the DoD dispenser (estimated to be 100 μL) is by far too high, even for on-line narrow-bore HPLC/MS. Reducing the dead volume by a factor of 10 (which would be possible with this commercial type of DoD generator), would still not be small enough to use for on-line capillary- respectively nanoHPLC/MS, as the chromatographic peak broadening would be much too big. On-line LC/MS coupling utilizing the interface in the microdroplet mode will require a dedicated droplet-on-demand dispenser having an ultralow dead volume to be able to work with packed capillaries at flow rates <1 μL/min. For this reason all chromatographic experiments (coupled via the new interface) were performed operating in continuous microbeam mode in conjunction with μHPLC equipment.

HPLC Application I: Peptide Mixture. An artificial mixture of seven peptides at different concentrations, (viz. Leu-Enk (14 pmol/μL), Met-Enk (1.4 pmol/μL), iPD1 (1.4 pmol/μL), Ang I and II (both 2.8 pmol/μL), Brad (28 pmol/μL), and Neu (1.4 pmol/μL)), was injected onto the microbore RP-column (C18, ID: 2.1 mm, length 150 mm) and eluted via linear 25 min gradient from 5 to 60% acetonitrile. Figure 5a shows the base peak intensity chromatogram (BPIC). For comparison, the UV-trace at 220 nm is displayed mirrored. The peptides have been eluted within a narrow time-window having retention times from 18 to 23 min. The partial overlapping of some peptide fractions is demonstrated by the overlay of reconstructed ion chromatograms (RIC's) shown in Figure 5b.

HPLC Application II: BSA Digest and PMF. Since mainly singly charged peptides are generated in AP-FL-IR-MALDI, we next tested whether it proves useful for proteomics by using a peptide mass fingerprint-like approach (PMF). Further, comparison of both ionization modes ((nano)ESI vs AP-FL-IR-MALDI) was done regarding its hardware similarities and its intrinsic differences in ionization:

Figure 6a shows the TICs of a μHPLC MS run (7.5 pmol tryptic BSA digest loaded on the microbore column) interfaced via AP-FL-IR-MALDI and mirrored for comparison the TIC trace obtained with nanoHPLC/MS (0.1 pmol tryptic BSA digest loaded on the

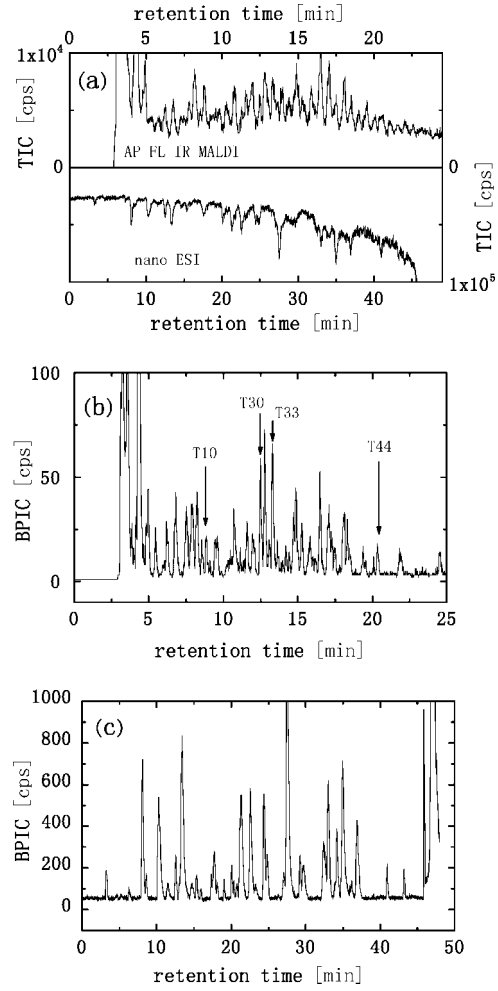

Figure 6. LC/MS of BSA digest. (a) TIC obtained with μHPLC AP-FL-IR-MALDI MS (7.5 pmol loaded on narrow-bore column (upper trace)) and nanoHPLC nanoESI MS (0.1 pmol loaded on capillary column (mirrored lower trace)), respectively. (b) BPIC of μHPLC AP-FL-IR-MALDI MS and (c) BPIC of nanoHPLC nanoESI MS.

capillary column) interfaced via nanoESI. Figures 6b and 6c show the base peak intensity chromatograms (BPIC) out of these TICs.

On the one hand, these on-line coupled LC/MS measurements in both ionization modes were conducted to demonstrate the possibility of switching between the two modes. As already mentioned in the introduction, commercially available on-line nanoESI emitters are well suited for the generation of continuous free liquid microbeams. Therefore, with some minor modifications, such an on-line nanoESI interface enables one to operate the mass spectrometer with these two different ionization modes using the same interface. In addition, switching over from nanoESI MS (high voltage on, laser off, low flow rate) to AP-FL-IR-MALDI MS (high voltage off, laser on, high flow rate) can be readily done within a short time.

On the other hand, the comparison of these measurements shows the performance differences between both modes, regarding concentration sensitivity, chemical background noise in the lower m/z region, and that at higher acetonitrile contents.

Apparently, the ESI measurement not only achieves an order of magnitude higher total ion current but also up to 10-fold higher signals of eluted fractions. The latter can, however, be well understood on the basis of the scaling law and similar concentra-

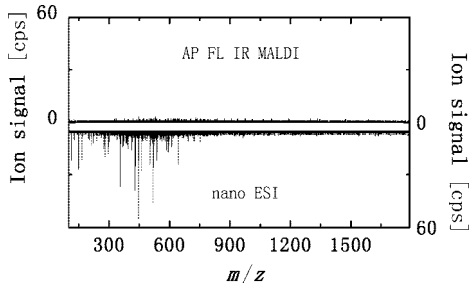

Figure 7. Comparison of mass spectra of the background corresponding to a single scan (i.e., 1 s acquisition time) of μHPLC AP-FL-IR-MALDI MS (upper trace) and nanoHPLC nanoESI MS (mirrored lower trace) of BSA tryptic digest.

tion sensitivity (and linearity) of the two ion sources whose concentration sensitivity limits happen to be equal and amount to several nM (nanomolar). Assuming, that the linear flow velocity is the same for both separations (about 1 mm/s), the scaling law predicts, for the same sample amount injected, about a 780-fold increase in sensitivity for the capillary column (0.075 mm ID) with respect to the 2.1 mm ID one. As the ratio of injected masses was (only) 75 (7.5 pmol:0.1 pmol; tryptic digested BSA), the above-mentioned factor of 10 is left (780:75), which means the peak sample concentration in the capillary column separation should be a factor of 10 higher as compared to the microbore column separation. Assuming now linearity of the nanoESI source, the expected 10-fold higher signals for nanoHPLC nanoESI MS compared to μHPLC AP-FL-IR-MALDI MS match the experimental findings.

Within the μHPLC AP-FL-IR-MALDI MS experiments, no noise signal increase is detected (respectively, no significant noise signal) over the whole acetonitrile gradient (cf. Figure 6a (upper trace: no baseline drift) and Figure 6b) and over the whole m/z-range (cf. Figure 7, upper trace). However, the nanoESI experiment generates quite high background signals at the lower m/z-range (cf. Figure 7, mirrored lower trace), and its BPIC shows outsized nonpeptide-derived signals at higher acetonitrile content (cf. Figure 6c, ACN > 60%, 45−50 min). A closer look at the mass spectra reveals that the AP-FL-IR-MALDI source produces significantly less background signal derived from, for example, solvent and residual salt clusters as well as contaminating peaks from air and solvent (Figure 7, upper trace). This extremely smooth baseline in the present μHPLC AP-FL-IR-MALDI MS experiments can be of great advantage, particularly, when dealing with analytes of small m/z-ratios (e.g., short peptides, small (organic) molecules, metabolites, drugs, etc.), which, in case of nanoESI MS, are not easy to detect because of its intrinsic noisy baseline in the region of low m/z-values (Figure 7, mirrored lower trace). The same argument would hold also for UV-MALDI MS which is prone to exhibit extensive matrix interferences (i.e., ion suppression and/or chemical noise), in particular, in the low mass range,[69,70] although some strategies devoted to reduce these effects have been recently devised.[71,72] This means, compared to (nano)ESI MS and UV-MALDI MS, AP-FL-IR-MALDI MS allows extremely low cutoff parameters, and therefore a high signal recognition, even for lowest signal intensities.

(69) Gobey, J.; M, C.; Janiszewski, J.; Covey, T.; Chau, T.; Kovarik, P.; Corr, J. *Anal. Chem.* **2005**, *77*, 5643–5654.

(70) Krutchinsky, A. N.; Chait, B. T. *J. Am. Soc. Mass Spectrom.* **2002**, *13*, 129–134.

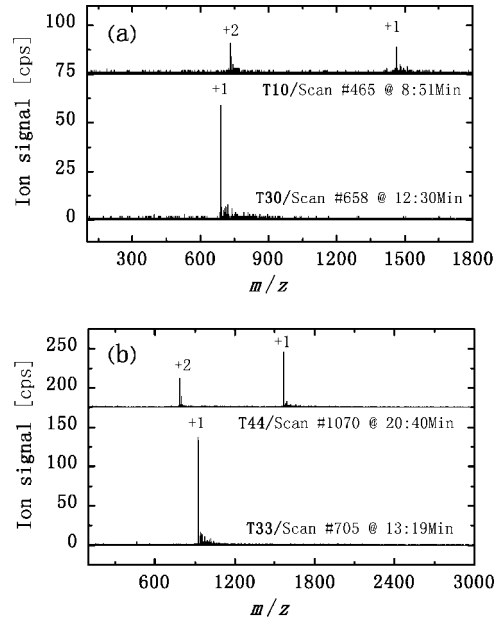

Figure 8. Four representative single scan mass spectra (1 s/scan) performed by μHPLC AP-FL-IR-MALDI MS generating PMFs of tryptic digested BSA. (a) 7.5 pmol BSA loaded: tryptic fragments T10 with two carbamidomethyl groups at cystein residues (TC*VADESHAGC*EK, M_r = 1348.54 + 2 × 57.02 = 1462.58), and T30 (AWSVAR, M_r = 688.36) are shown. (b) 37.5 pmol BSA loaded: tryptic fragments T44 (DAFLGSFLYEYSR, M_r = 1566.73) and T33 (AEFVEVTK, M_r = 921.48) are illustrated.

PMF data evaluation, including data processing and peak picking, was done as described in the Experimental Section. Tables 1 and 2 summarize the PMF search results on AP-FL-IR-MALDI. The tables also introduce the ratio of the matched peptides versus the entire number of values, subjected to the search (η) as a criterion of the data quality of the search. Using peak picking criteria of r = 6 cps for 7.5 pmol of tryptic digested BSA absolute loaded on the column, 54 peptides (from 129 peaks) were assigned as tryptic peptides of BSA. This corresponds to sequence coverage of 71% and MOWSE[56] scores above 300. For 37.5 pmol of tryptic digested BSA absolute loaded on the column, even up to 93% sequence coverage could be reached (cf. Table 2). These data demonstrate that AP-FL-IR-MALDI is highly useful for the on-line coupled fast peptide mass fingerprint analysis of complex mixtures. We envision such a setup to be highly suitable for the rapid mapping of proteins on routine basis where high sequence coverage is needed. This includes (i) routine identification of overexpressed proteins, (ii) in depth PMF for definition of the N- and C-terminus of truncated or endo(exo-) proteolytically processed proteins, and (iii) in depth PMF for the detection of post-translational modifications. A similar set up using MALDI-ToF is much more time-consuming, as the chromatographic separation of the mixture has to be performed off-line prior to MS analysis, utilizing a standard MALDI instrument.

Some final points which deserve to be mentioned are as follows:

Concerning MS/MS investigations, unlike MALDI but similar to ESI, the presence of higher charge states in AP-FL-IR-MALDI (Figure 8) would allow to perform MS/MS using $[M + 2H]^{2+}$, which are believed to generate the most informative highest

quality tandem mass spectra.[73] It turned out that smaller peptides (<1000 Da) were mainly singly charged, while larger peptides (>1000 Da) appeared also as doubly charged species, though typically at slightly lower abundance than the singly charged ones. Interestingly, the high abundance of singly charged peptides in AP-FL-IR-MALDI MS opens thus the opportunity for their successful fragmentation, despite of the unfavorable fragment ion yields.

On acquisition of fragmentation patterns of both single- and double-charge precursor ions, complementary information can be obtained.[73,74] The possibility to increase the fragmentation efficiency for singly charged ions will be investigated on a QqTOF hybrid tandem mass spectrometer (Applied Biosystems MDS/Sciex, Canada), which allows higher collision energies because of its orthogonal MALDI source option and using Argon as collision gas.

An important point in LC/MS studies is the robust and reliable operation of an ion source. In electrospray processes, for instance, the conditions for stable operation (in cone-jet mode) may not be always fulfilled upon gradient-based elution, an issue addressed recently by Marginean et al.[75] Similarly, the presence of an organic modifier (e.g., ACN) changes somewhat the absorption coefficient of the IR radiation in the μHPLC AP-FL-IR-MALDI MS experiment. As a consequence it may have impact on both the disintegration process of the liquid beam and the subsequent desolvation. Fortunately, only moderate dependence of the MS signal on the composition of the mobile phase was found. Thus, for instance, varying the composition of the solvent from pure 0.1% FA_{aq} to 50/50 ACN/0.1% FA_{aq}, the bradykinin signal increased about 25% (data not shown).

Finally, using a homogeneous matrix (i.e., liquid), shot-to-shot (or "spot-to-spot") reproducibility should be significantly better than that achieved in UV/IR-MALDI with solid matrices, where small unevenly distributed crystallites are essential for obtaining high quality mass spectra.[76,77]

CONCLUSIONS

In this study, a new concept of an ion source working at ambient conditions has been presented. The ion source is based on using a continuous liquid microbeam, whose homogeneous part (i.e., before disintegration into droplets) is irradiated by a nanosecond radiation of an IR OPO. Adapting this source to a Micromass Q-Tof mass spectrometer has been facilitated by the open construction of the ESI ion source of this instrument. No particular modifications were required to operate the new ion source. Yet, also other mass spectrometers could be equipped with such an ion source (as already mentioned, the implementation of this interface to the QSTAR XL QqTof hybrid tandem mass spectrometer from Applied Biosystems MDS/Sciex is an ongoing project).

This paper is devoted to the (first) application of the continuous source to the mass analysis of different peptide samples in the flow injection mode. The sensitivity of 17 fmol/scan and a (detector-limited) linearity range spanning 2 orders of magnitude have been determined. Liquid delivery based on a droplet-on-demand setup improved the sample consumption by about 3 orders of magnitude (20 attomole) upon preserving the linearity behavior between sample concentration and ion signal.

Concerning liquid chromatography, there are still many instances where the use of conventional-bore chromatographic methods is warranted. In many cases, where sample amount is not an issue, it is always advantageous to use robust and reproducible standard LC equipment for columns from analytical down to the microbore dimension[78] and to avoid the intrinsic problems arising with further miniaturization. In addition, there are circumstances under which it is necessary to utilize larger injection volumes of a reconstituted physiological sample to introduce sufficient quantities of isolated trace level analyte into the LC/MS system.[79]

The present version is well suited for standard HPLC applications, where flow rates higher than 100 μL/min are required. The utility as an on-line LC/MS detector has been demonstrated, in particular, by performing a peptide mass mapping on BSA tryptic digest.

Further development of a droplet-on-demand version of the apparatus with attomole sensitivity at flow rates in the sub-μL/min range is indeed promising for applications dealing with limited sample amount. Future experiments will explore the nanoHPLC combined with the MS/MS capabilities, on-line coupled via AP-FL-IR-MALDI. It will be highly interesting to see how tryptic peptide mixtures derived from (post-translational) modified proteins perform in AP-FL-IR-MALDI. Furthermore, we suggest that this ionization method will prove highly useful in the analysis of glycans and nucleic acids, as in particular longer nucleic acid stretches that show poor behavior in MALDI and/or generate multiple charged species in ESI. The performance of the AP-FL-IR-MALDI MS in the negative ion mode is already under investigation.

ACKNOWLEDGMENT

Financial support from the Deutsche Forschungsgemeinschaft (DFG) through the SFB 755 and the GK 782, as well as from the Max Planck Society (MPG) is gratefully acknowledged. The authors do not claim competing financial interests.

SUPPORTING INFORMATION AVAILABLE

Further details are given in Tables S-1 and S-2, and Figure S-1. This material is available free of charge via the Internet at http://pubs.acs.org.

Received for review September 3, 2008. Accepted November 11, 2008.

AC801863P

(71) Guo, Z.; He, L. *Anal. Bioanal. Chem.* **2007**, *387*, 1939–1944.
(72) Donegan, M.; Tomlinson, A. J.; Nair, H.; Juhacz, P. *Rapid Commun. Mass Spectrom.* **2004**, *18*, 1885–1888.
(73) Ashcroft, A. E. *Nat. Prod. Rep.* **2003**, *20*, 202–215.
(74) Wattenberg, A.; Organ, A. J.; Schneider, K.; Tyldesley, R.; Bordoli, R. S.; Bateman, R. H. *J. Am. Soc. Mass Spectrom.* **2002**, *13*, 772–783.
(75) Marginean, I.; Kelly, R. T.; Page, J. S.; Tang, K.; Smith, R. D. *Anal. Chem.* **2007**, *79*, 8030–8036.
(76) Cohen, S. L.; Chait, B. T. *Anal. Chem.* **1996**, *68*, 31–37.
(77) Schwartz, S. A.; Reyzer, M. L.; Caprioli, R. M. *J. Mass Spectrom.* **2003**, *38*, 699–708.
(78) Rapp, E.; Tallarek, U. *J. Sep. Sci.* **2003**, *26*, 453–470.
(79) Gangl, E. T.; Annan, M.; Spooner, N.; Vouros, P. *Anal. Chem.* **2001**, *73*, 5635–5644.